

Coherent Soft Particle Production in Z Decays into Three Jets

DELPHI Collaboration

Abstract

Low-energy particle production perpendicular to the event plane in three-jet events produced in Z decays in e^+e^- annihilation is measured and compared to that perpendicular to the event axis in two-jet events. The topology dependence of the hadron production ratio is found to agree with a leading-order QCD prediction. This agreement and especially the need for the presence of a destructive interference term gives evidence for the coherent nature of gluon radiation. Hadron production in three-jet events is found to be directly proportional to a single topological scale function of the inter-jet angles. The slope of the dependence of the multiplicity with respect to the topological scale was measured to be:

$$2.211 \pm 0.014(\text{stat.}) \pm 0.053(\text{syst.})$$

in good agreement with the expectation given by the colour-factor ratio $C_A/C_F = 9/4$. This result strongly supports the assumption of local parton-hadron duality, LPHD, at low hadron momentum.

(Accepted by Physics Letters B)

J.Abdallah²⁵, P.Abreu²², W.Adam⁵¹, P.Adzic¹¹, T.Albrecht¹⁷, T.Alderweireld², R.Aleman-Fernandez⁸, T.Allmendinger¹⁷, P.P.Allport²³, U.Amaldi²⁹, N.Amapane⁴⁵, S.Amato⁴⁸, E.Anashkin³⁶, A.Andreazza²⁸, S.Andringa²², N.Anjos²², P.Antilogus²⁵, W-D.Apel¹⁷, Y.Arnoud¹⁴, S.Ask²⁶, B.Asman⁴⁴, J.E.Augustin²⁵, A.Augustinus⁸, P.Baillon⁸, A.Ballestrero⁴⁶, P.Bambade²⁰, R.Barbier²⁷, D.Bardin¹⁶, G.Barker¹⁷, A.Baroncelli³⁹, M.Battaglia⁸, M.Baubillier²⁵, K-H.Becks⁵³, M.Begalli⁶, A.Behrmann⁵³, E.Ben-Haim²⁰, N.Benekos³², A.Benvenuti⁵, C.Berat¹⁴, M.Berggren²⁵, L.Berntzon⁴⁴, D.Bertrand², M.Besancon⁴⁰, N.Besson⁴⁰, D.Bloch⁹, M.Blom³¹, M.Bluj⁵², M.Bonesini²⁹, M.Boonekamp⁴⁰, P.S.L.Booth²³, G.Borisov²¹, O.Botner⁴⁹, B.Bouquet²⁰, T.J.V.Bowcock²³, I.Boyko¹⁶, M.Bracko⁴³, R.Brenner⁴⁹, E.Brodet³⁵, P.Bruckman¹⁸, J.M.Brunet⁷, L.Bugge³³, P.Buschmann⁵³, M.Calvi²⁹, T.Camporesi⁸, V.Canale³⁸, F.Carena⁸, N.Castro²², F.Cavallo⁵, M.Chapkin⁴², Ph.Charpentier⁸, P.Checchia³⁶, R.Chierici⁸, P.Chliapnikov⁴², J.Chudoba⁸, S.U.Chung⁸, K.Cieslik¹⁸, P.Collins⁸, R.Contri¹³, G.Cosme²⁰, F.Cossutti⁴⁷, M.J.Costa⁵⁰, D.Crennell³⁷, J.Cuevas³⁴, J.D'Hondt², J.Dalmau⁴⁴, T.da Silva⁴⁸, W.Da Silva²⁵, G.Della Ricca⁴⁷, A.De Angelis⁴⁷, W.De Boer¹⁷, C.De Clercq², B.De Lotto⁴⁷, N.De Maria⁴⁵, A.De Min³⁶, L.de Paula⁴⁸, L.Di Ciaccio³⁸, A.Di Simone³⁹, K.Doroba⁵², J.Drees^{53,8}, M.Dris³², G.Eigen⁴, T.Ekelof⁴⁹, M.Ellert⁴⁹, M.Elsing⁸, M.C.Espirito Santo²², G.Fanourakis¹¹, D.Fassouliotis^{11,3}, M.Feindt¹⁷, J.Fernandez⁴¹, A.Ferrer⁵⁰, F.Ferro¹³, U.Flammeyer⁵³, H.Foeth⁸, E.Fokitis³², F.Fulda-Quenzer²⁰, J.Fuster⁵⁰, M.Gandelman⁴⁸, C.Garcia⁵⁰, Ph.Gavillet⁸, E.Gazis³², R.Gokieli^{8,52}, B.Golob⁴³, G.Gomez-Ceballos⁴¹, P.Goncalves²², E.Graziani³⁹, G.Grosdidier²⁰, K.Grzelak⁵², J.Guy³⁷, C.Haag¹⁷, A.Hallgren⁴⁹, K.Hamacher⁵³, K.Hamilton³⁵, S.Haug³³, F.Hauler¹⁷, V.Hedberg²⁶, M.Hennecke¹⁷, H.Herr⁸, J.Hoffman⁵², S-O.Holmgren⁴⁴, P.J.Holt⁸, M.A.Houlden²³, K.Hultqvist⁴⁴, J.N.Jackson²³, G.Jarlskog²⁶, P.Jarry⁴⁰, D.Jeans³⁵, E.K.Johansson⁴⁴, P.D.Johansson⁴⁴, P.Jonsson²⁷, C.Joram⁸, L.Jungermann¹⁷, F.Kapusta²⁵, S.Katsanevas²⁷, E.Katsoufis³², G.Kernel⁴³, B.P.Kersevan^{8,43}, U.Kerzel¹⁷, A.Kiiskinen¹⁵, B.T.King²³, N.J.Kjaer⁸, P.Kluit³¹, P.Kokiniias¹¹, C.Kourkoumelis³, O.Kouznetsov¹⁶, Z.Krumstein¹⁶, M.Kucharczyk¹⁸, J.Lamsa¹, G.Leder⁵¹, F.Ledroit¹⁴, L.Leinonen⁴⁴, R.Leitner³⁰, J.Lemonne², V.Lepeltier²⁰, T.Lesiak¹⁸, W.Liebig⁵³, D.Liko⁵¹, A.Lipniacka⁴⁴, J.H.Lopes⁴⁸, J.M.Lopez³⁴, D.Loukas¹¹, P.Lutz⁴⁰, L.Lyons³⁵, J.MacNaughton⁵¹, A.Malek⁵³, S.Maltesos³², F.Mandl⁵¹, J.Marco⁴¹, R.Marco⁴¹, B.Marechal⁴⁸, M.Margoni³⁶, J-C.Marin⁸, C.Mariotti⁸, A.Markou¹¹, C.Martinez-Rivero⁴¹, J.Masik¹², N.Mastroiannopoulos¹¹, F.Matorras⁴¹, C.Matteuzzi²⁹, F.Mazzucato³⁶, M.Mazzucato³⁶, R.Mc Nulty²³, C.Meroni²⁸, E.Migliore⁴⁵, W.Mitaroff⁵¹, U.Mjoernmark²⁶, T.Moa⁴⁴, M.Moch¹⁷, K.Moenig^{8,10}, R.Monge¹³, J.Montenegro³¹, D.Moraes⁴⁸, S.Moreno²², P.Moretini¹³, U.Mueller⁵³, K.Muenich⁵³, M.Mulders³¹, L.Mundim⁶, W.Murray³⁷, B.Muryn¹⁹, G.Myatt³⁵, T.Myklebust³³, M.Nassiakou¹¹, F.Navarria⁵, K.Nawrocki⁵², R.Nicolaidou⁴⁰, M.Nikolenko^{16,9}, A.Oblakowska-Mucha¹⁹, V.Obraztsov⁴², A.Olshevski¹⁶, A.Onofre²², R.Orava¹⁵, K.Osterberg¹⁵, A.Ouraou⁴⁰, A.Oyanguren⁵⁰, M.Paganoni²⁹, S.Paiano⁵, J.P.Palacios²³, H.Palka¹⁸, Th.D.Papadopoulou³², L.Pape⁸, C.Parkes²⁴, F.Parodi¹³, U.Parzefall⁸, A.Passeri³⁹, O.Passon⁵³, L.Peralta²², V.Perepelitsa⁵⁰, A.Perrotta⁵, A.Petrolini¹³, J.Piedra⁴¹, L.Pieri³⁹, F.Pierre⁴⁰, M.Pimenta²², E.Piotto⁸, T.Podobnik⁴³, V.Poireau⁸, M.E.Pol⁶, G.Polok¹⁸, P.Poropat⁴⁷, V.Pozdniakov¹⁶, N.Pukhaeva^{2,16}, A.Pullia²⁹, J.Rames¹², L.Ramler¹⁷, A.Read³³, P.Rebecchi⁸, J.Rehn¹⁷, D.Reid³¹, R.Reinhardt⁵³, P.Renton³⁵, F.Richard²⁰, J.Ridky¹², M.Rivero⁴¹, D.Rodriguez⁴¹, A.Romero⁴⁵, P.Ronchese³⁶, P.Roudeau²⁰, T.Rovelli⁵, V.Ruhlmann-Kleider⁴⁰, D.Ryabtchikov⁴², A.Sadovsky¹⁶, L.Salmi¹⁵, J.Salt⁵⁰, A.Savoy-Navarro²⁵, U.Schwickerath⁸, A.Segar³⁵, R.Sekulin³⁷, M.Siebel⁵³, A.Sisakian¹⁶, G.Smadja²⁷, O.Smirnova²⁶, A.Sokolov⁴², A.Sopczak²¹, R.Sosnowski⁵², T.Spassov⁸, M.Stanitzki¹⁷, A.Stocchi²⁰, J.Strauss⁵¹, B.Stugu⁴, M.Szczekowski⁵², M.Szeptycka⁵², T.Szumlak¹⁹, T.Tabarelli²⁹, A.C.Taffard²³, F.Tegenfeldt⁴⁹, J.Timmermans³¹, L.Tkatchev¹⁶, M.Tobin²³, S.Todorovova¹², B.Tome²², A.Tonazzo²⁹, P.Tortosa⁵⁰, P.Travnicek¹², D.Treille⁸, G.Tristram⁷, M.Trochimczuk⁵², C.Troncon²⁸, M-L.Turluer⁴⁰, I.A.Tyapkin¹⁶, P.Tyapkin¹⁶, S.Tzamarias¹¹, V.Uvarov⁴², G.Valenti⁵, P.Van Dam³¹, J.Van Eldik⁸, A.Van Lysebetten², N.van Remortel², I.Van Vulpen⁸, G.Vegni²⁸, F.Veloso²², W.Venus³⁷, P.Verdier²⁷, V.Verzi³⁸, D.Vilanova⁴⁰, L.Vitale⁴⁷, V.Vrba¹², H.Wahlen⁵³, A.J.Washbrook²³, C.Weiser¹⁷,

D.Wicke⁸, J.Wickens², G.Wilkinson³⁵, M.Winter⁹, M.Witek¹⁸, O.Yushchenko⁴², A.Zalewska¹⁸, P.Zalewski⁵²,
D.Zavrtanik⁴³, V.Zhuravlov¹⁶, N.I.Zimin¹⁶, A.Zintchenko¹⁶, M.Zupan¹¹

-
- ¹Department of Physics and Astronomy, Iowa State University, Ames IA 50011-3160, USA
²Physics Department, Universiteit Antwerpen, Universiteitsplein 1, B-2610 Antwerpen, Belgium
and IIHE, ULB-VUB, Pleinlaan 2, B-1050 Brussels, Belgium
and Faculté des Sciences, Univ. de l'Etat Mons, Av. Maistriau 19, B-7000 Mons, Belgium
³Physics Laboratory, University of Athens, Solonos Str. 104, GR-10680 Athens, Greece
⁴Department of Physics, University of Bergen, Allégaten 55, NO-5007 Bergen, Norway
⁵Dipartimento di Fisica, Università di Bologna and INFN, Via Irnerio 46, IT-40126 Bologna, Italy
⁶Centro Brasileiro de Pesquisas Físicas, rua Xavier Sigaud 150, BR-22290 Rio de Janeiro, Brazil
and Depto. de Física, Pont. Univ. Católica, C.P. 38071 BR-22453 Rio de Janeiro, Brazil
and Inst. de Física, Univ. Estadual do Rio de Janeiro, rua São Francisco Xavier 524, Rio de Janeiro, Brazil
⁷Collège de France, Lab. de Physique Corpusculaire, IN2P3-CNRS, FR-75231 Paris Cedex 05, France
⁸CERN, CH-1211 Geneva 23, Switzerland
⁹Institut de Recherches Subatomiques, IN2P3 - CNRS/ULP - BP20, FR-67037 Strasbourg Cedex, France
¹⁰Now at DESY-Zeuthen, Platanenallee 6, D-15735 Zeuthen, Germany
¹¹Institute of Nuclear Physics, N.C.S.R. Demokritos, P.O. Box 60228, GR-15310 Athens, Greece
¹²FZU, Inst. of Phys. of the C.A.S. High Energy Physics Division, Na Slovance 2, CZ-180 40, Praha 8, Czech Republic
¹³Dipartimento di Fisica, Università di Genova and INFN, Via Dodecaneso 33, IT-16146 Genova, Italy
¹⁴Institut des Sciences Nucléaires, IN2P3-CNRS, Université de Grenoble 1, FR-38026 Grenoble Cedex, France
¹⁵Helsinki Institute of Physics, P.O. Box 64, FIN-00014 University of Helsinki, Finland
¹⁶Joint Institute for Nuclear Research, Dubna, Head Post Office, P.O. Box 79, RU-101 000 Moscow, Russian Federation
¹⁷Institut für Experimentelle Kernphysik, Universität Karlsruhe, Postfach 6980, DE-76128 Karlsruhe, Germany
¹⁸Institute of Nuclear Physics, Ul. Kawary 26a, PL-30055 Krakow, Poland
¹⁹Faculty of Physics and Nuclear Techniques, University of Mining and Metallurgy, PL-30055 Krakow, Poland
²⁰Université de Paris-Sud, Lab. de l'Accélérateur Linéaire, IN2P3-CNRS, Bât. 200, FR-91405 Orsay Cedex, France
²¹School of Physics and Chemistry, University of Lancaster, Lancaster LA1 4YB, UK
²²LIP, IST, FCUL - Av. Elias Garcia, 14-1º, PT-1000 Lisboa Codex, Portugal
²³Department of Physics, University of Liverpool, P.O. Box 147, Liverpool L69 3BX, UK
²⁴Dept. of Physics and Astronomy, Kelvin Building, University of Glasgow, Glasgow G12 8QQ
²⁵LPNHE, IN2P3-CNRS, Univ. Paris VI et VII, Tour 33 (RdC), 4 place Jussieu, FR-75252 Paris Cedex 05, France
²⁶Department of Physics, University of Lund, Sölvegatan 14, SE-223 63 Lund, Sweden
²⁷Université Claude Bernard de Lyon, IPNL, IN2P3-CNRS, FR-69622 Villeurbanne Cedex, France
²⁸Dipartimento di Fisica, Università di Milano and INFN-MILANO, Via Celoria 16, IT-20133 Milan, Italy
²⁹Dipartimento di Fisica, Univ. di Milano-Bicocca and INFN-MILANO, Piazza della Scienza 2, IT-20126 Milan, Italy
³⁰IPNP of MFF, Charles Univ., Areal MFF, V Holesovickach 2, CZ-180 00, Praha 8, Czech Republic
³¹NIKHEF, Postbus 41882, NL-1009 DB Amsterdam, The Netherlands
³²National Technical University, Physics Department, Zografou Campus, GR-15773 Athens, Greece
³³Physics Department, University of Oslo, Blindern, NO-0316 Oslo, Norway
³⁴Dpto. Física, Univ. Oviedo, Avda. Calvo Sotelo s/n, ES-33007 Oviedo, Spain
³⁵Department of Physics, University of Oxford, Keble Road, Oxford OX1 3RH, UK
³⁶Dipartimento di Fisica, Università di Padova and INFN, Via Marzolo 8, IT-35131 Padua, Italy
³⁷Rutherford Appleton Laboratory, Chilton, Didcot OX11 0QX, UK
³⁸Dipartimento di Fisica, Università di Roma II and INFN, Tor Vergata, IT-00173 Rome, Italy
³⁹Dipartimento di Fisica, Università di Roma III and INFN, Via della Vasca Navale 84, IT-00146 Rome, Italy
⁴⁰DAPNIA/Service de Physique des Particules, CEA-Saclay, FR-91191 Gif-sur-Yvette Cedex, France
⁴¹Instituto de Física de Cantabria (CSIC-UC), Avda. los Castros s/n, ES-39006 Santander, Spain
⁴²Inst. for High Energy Physics, Serpukov P.O. Box 35, Protvino, (Moscow Region), Russian Federation
⁴³J. Stefan Institute, Jamova 39, SI-1000 Ljubljana, Slovenia and Laboratory for Astroparticle Physics,
Nova Gorica Polytechnic, Kostanjevska 16a, SI-5000 Nova Gorica, Slovenia,
and Department of Physics, University of Ljubljana, SI-1000 Ljubljana, Slovenia
⁴⁴Fysikum, Stockholm University, Box 6730, SE-113 85 Stockholm, Sweden
⁴⁵Dipartimento di Fisica Sperimentale, Università di Torino and INFN, Via P. Giuria 1, IT-10125 Turin, Italy
⁴⁶INFN, Sezione di Torino, and Dipartimento di Fisica Teorica, Università di Torino, Via P. Giuria 1,
IT-10125 Turin, Italy
⁴⁷Dipartimento di Fisica, Università di Trieste and INFN, Via A. Valerio 2, IT-34127 Trieste, Italy
and Istituto di Fisica, Università di Udine, IT-33100 Udine, Italy
⁴⁸Univ. Federal do Rio de Janeiro, C.P. 68528 Cidade Univ., Ilha do Fundão BR-21945-970 Rio de Janeiro, Brazil
⁴⁹Department of Radiation Sciences, University of Uppsala, P.O. Box 535, SE-751 21 Uppsala, Sweden
⁵⁰IFIC, Valencia-CSIC, and D.F.A.M.N., U. de Valencia, Avda. Dr. Moliner 50, ES-46100 Burjassot (Valencia), Spain
⁵¹Institut für Hochenergiephysik, Österr. Akad. d. Wissensch., Nikolsdorfergasse 18, AT-1050 Vienna, Austria
⁵²Inst. Nuclear Studies and University of Warsaw, Ul. Hoza 69, PL-00681 Warsaw, Poland
⁵³Fachbereich Physik, University of Wuppertal, Postfach 100 127, DE-42097 Wuppertal, Germany

1 Introduction

Quantum-mechanical interference effects are basic to the gauge theories of fundamental interactions such as Quantum Chromodynamics, QCD. The probabilistic Parton Model of strong interactions, however, neglecting interference effects still successfully describes many processes as an incoherent sum of the individual sub-processes. In fact it has proved difficult to show strong-interaction interference effects in high-energy inelastic processes like e^+e^- annihilation, deep-inelastic scattering or $p\bar{p}$ interactions. Evidence for coherent soft gluon emission in multiparticle production comes from the necessity to include angular ordering in the fragmentation models in order to describe the energy dependence of hard interactions, from the so called *hump backed plateau* in the logarithmic scaled-momentum spectrum of hadrons due to the suppression of low-energy particle production, and from the string-effect in three-jet events in e^+e^- annihilation explained by destructive interference. For a comprehensive review see [1].

Arguments against the conclusiveness of these verifications of coherence effects have been raised, however. Incoherent fragmentation models involving a large number of parameters allow for a sufficient description of the data at least at fixed centre-of-mass energy [2]. The hadronic momentum spectrum and the energy dependence of the peak of this distribution may also be accounted for when assuming a non-minimal phase-space structure [3]. The string-effect measurements, except for symmetric topologies [4,1], are also influenced by boost effects.

In this letter evidence for quantum-mechanical interference or colour coherence is presented from the comparison of low-energy hadron production perpendicular to the event plane of three-jet events and the event axis of two-jet events, respectively. Similarly to the string-effect, in this case the presence of destructive interference is expected. Presuming colour coherence, the measurement is also directly sensitive to the colour of the underlying partons, q , \bar{q} and g . The ratio of the colour charges or the colour-factors for gluons and quarks, C_A/C_F , can be verified directly from the dependence of the hadron production on the three-jet topology.

This letter is organised as follows. In Section 2 a basic description of the theoretical formulae and the ideas underlying this measurement are given. Section 3 gives an overview of the data, selections and corrections applied and describes the measurement. In Section 4 results on the hadron multiplicity observed in cones oriented perpendicular to the event plane of three-jet events and the event axis of two-jet events, respectively, are presented and conclusions are given.

2 Motivation and Theoretical Basis of the Measurement

The hadronisation process is believed to commence with the radiation of soft gluons from the initial hard partons. Due to the higher colour charge of gluons compared to quarks, soft gluon radiation and consequently hadron production is expected to be increased in the high energy limit by the gluon to quark colour-factor ratio $C_A/C_F = 9/4$. This simple expectation is perturbed for hadrons sharing a large fraction of the energy of the underlying parton. Leading-particle effects become evident and, as such particles are created last in time [5], effects due to energy conservation are important. The latter influence is stronger for gluon jets due to the more copious particle production.

When a radiated hard gluon stays close to the radiating quark, additional soft gluons may be unable to resolve the individual colour charges of the close-by partons. In this limit only coherent radiation off the parton ensemble, that is from the colour charge of the initial quark occurs. This fundamental effect also leads to the angular-ordering property of soft gluon emission.

Coherence effects should be best visible for low-energy hadrons emitted perpendicularly to the radiating partons as these particles cannot be assigned to a specific jet and have a poor resolution power for close-by colour charges.

The cross-section for soft-gluon radiation in $(q\bar{q}g)$ three-jet events has been calculated in [6]. It varies strongly as a function of the three-jet topology. In contrast to many other event characteristics, the soft radiation out of the $q\bar{q}g$ plane is dominated in the perturbative calculation by the leading-order contribution which takes a particularly simple form [7]:

$$d\sigma_3 = d\sigma_2 \cdot \frac{C_A}{C_F} \cdot r_t \quad r_t = \frac{1}{4} \left\{ \widehat{qg} + \widehat{\bar{q}g} - \frac{1}{N_c^2} \widehat{q\bar{q}} \right\} \quad (1)$$

with the so called *antenna function*

$$\widehat{ij} = 1 - \cos \theta_{ij} = 2 \sin^2 \frac{\theta_{ij}}{2} \quad .$$

Here $d\sigma_3$ is the cross-section for soft gluon emission perpendicular to the $q\bar{q}g$ plane, $d\sigma_2$ the corresponding cross-section for emission perpendicular to the two-jet event $(q\bar{q})$ axis, and θ_{ij} denotes the angle between the partons i and j . The complete topology dependence can be factorised in the topological term r_t which, multiplied by the energy, obviously plays the rôle of the evolution scale of the low energy hadron multiplicity.

Equation 1 interpolates between the two cases in which $q\bar{q}g$ events appear as two-jet events. For gluon radiation parallel to the quark (or antiquark) $r_t = 4/9$ and $d\sigma_3 = d\sigma_2$, as soft particles cannot resolve the individual colour charges of the quark and the gluon. In the case where the gluon recoils with respect to the quark antiquark pair $r_t = 1$. This case is similar to an initial two-gluon state forming a colour singlet and $d\sigma_3 = C_A/C_F \cdot d\sigma_2$. The term inversely proportional to the square of the number of colours, $N_c = 3$, in r_t is due to destructive interference and provides an additional suppression of particle production on top of the boost effects caused by the string-like topology in general three-jet events.

The interest of the measurement presented in this paper is:

- the experimental test of the predicted topology dependence manifesting the coherent nature of hadron production,
- the verification of the $1/N_c^2$ term as direct evidence for the negative interference term beyond the probabilistic parton cascade and
- the measurement of the slope of the homogenous straight-line given by Equation 1 and thereby the verification of the colour-factor ratio C_A/C_F .

In order to verify the above predictions experimentally, charged-particle production has been studied in cones with $\vartheta_{\text{cone}} = 30^\circ$ half opening angle situated perpendicular to both sides of the three-jet plane or the two-jet event axis. For two-jet events the azimuthal orientation of the cones is taken randomly. In order to distinguish events with two, three and four or more jets the angular ordered Durham (aoD) algorithm is used with a jet-resolution parameter $y_{\text{cut}} = 0.015$. The aoD algorithm corresponds to the Cambridge algorithm without soft freezing [8]. It has been chosen as it is expected to lead to optimal reconstruction of jet directions but to avoid complications due to soft

freezing. The choice of a fixed jet-resolution is necessary as the leading-order prediction of Equation 1, applies to two- and three-jet events. Consequently, events with less than two or more than three jets are explicitly excluded from the analysis.

These experimental choices, made in order to approximate the theoretical prediction, imply systematic uncertainties in the data-to-theory comparison. The possible systematic variations of the data were assessed by varying the cone opening angle in the range $20^\circ \leq \vartheta_{\text{cone}} \leq 40^\circ$ and the jet-resolution in the range $0.01 \leq y_{\text{cut}} \leq 0.02$. Moreover the Cambridge [8] and Durham [9] algorithms were used alternatively. The uncertainty of the leading-order prediction, Equation 1, is not specified in [7] and, consequently, is not included in the uncertainties of the derived quantities quoted below.

In order to compare the prediction, Equation 1, to the data directly, the prediction is evaluated for each of the possible assignments of the gluon to the three jets. Finally, the three results are averaged with each assignment being weighted according to the respective three-jet matrix element. The topological term r_t in principle varies between $4/9 \sim 0.44$ and 1. In this analysis the lower limit is $r_t^{\text{min}} \sim 0.5$, as the cut in the jet-resolution implies a minimum angle between the gluon and a quark. As gluon-jets stay unidentified and gluon radiation at low angles dominates, the maximum weighted average value of r_t , $r_t^{\text{max}} \sim 0.71$ is obtained for fully-symmetric three-jet events.

3 Data and Data Analysis

This analysis is based on hadronic Z decays collected in the years 1992 to 1995 with the DELPHI detector at the LEP e^+e^- collider at CERN. The DELPHI detector was a hermetic collider detector with a solenoidal magnetic field, extensive tracking facilities including a micro-vertex detector, electromagnetic and hadronic calorimetry as well as strong particle identification capabilities. The detector and its performance are described in detail elsewhere [10,11].

In order to select well-measured particles originating from the interaction point, the cuts shown in Table 1 were applied to the measured tracks and electromagnetic or hadronic calorimeter clusters. Here p and E denote the particle's momentum and energy, ϑ_{polar} denotes the polar angle with respect to the beam, ϵ_k is the distance of closest approach to the interaction point in the plane perpendicular to (xy) or along (z) the beam, respectively, L_{track} is the measured track length. E_{HPC} (E_{EMF}) denotes the energy of a cluster as measured with the barrel (forward) electromagnetic calorimeter, respectively, and E_{HAC} the cluster energy measured by the hadronic calorimeter.

The general event cuts shown in Table 2 select hadronic decays of the Z and suppress background from leptonic Z decays, $\gamma\gamma$ interactions or beam-gas interactions to a negligible level. Further reduction of background is achieved by the jet-selection cuts given also in Table 2. The cut variables are the visible charged energy, $E_{\text{charged}}^{\text{total}}$ and $E_{\text{charged}}^{\text{hemisph.}}$, observed in the event or in one event hemisphere, respectively. Event hemispheres are defined by the plane perpendicular to the sphericity axis. The polar angle of this axis with respect to the beam is $\vartheta_{\text{sphericity}}$ and N_{charged} is the observed charged multiplicity. Events are discarded, if they contain charged particles with momenta above the kinematic limit.

Events are then clustered into jets using the aoD (or, alternatively, the Durham or Cambridge) algorithm. The three-jet event quality requirements also shown in Table 2 assure well-measured jets. Here θ_i denotes the angle between the two jets opposite to jet i , ϑ_{jet} the polar angle of a jet and $E_{\text{visible}}/\text{jet}$ the total visible energy per jet. The sequence number i of a jet is given by ordering the jets with decreasing jet energy

variable	cut
p	$\geq 0.4 \text{ GeV}$
ϑ_{polar}	$20^\circ - 160^\circ$
ϵ_{xy}	$\leq 5 \text{ cm}$
ϵ_z	$\leq 10 \text{ cm}$
L_{track}	$\geq 30 \text{ cm}$
$\Delta p/p$	$\leq 100\%$
E_{HPC}	$0.5 \text{ GeV} - 50 \text{ GeV}$
E_{EMF}	$0.5 \text{ GeV} - 50 \text{ GeV}$
E_{HAC}	$1 \text{ GeV} - 50 \text{ GeV}$

Table 1: Selection cuts applied to charged-particle tracks and to calorimeter clusters.

variable	cut
general events	
$E_{\text{charged}}^{\text{hemisph.}}$	$\geq 0.03 \cdot \sqrt{s}$
$E_{\text{charged}}^{\text{total}}$	$\geq 0.12 \cdot \sqrt{s}$
N_{charged}	≥ 5
$\vartheta_{\text{sphericity}}$	$30^\circ - 150^\circ$
p_{max}	45 GeV
three-jet events	
$\sum_{i=1}^3 \theta_i$	$> 355^\circ$
$E_{\text{visible}}/\text{jet}$	$\geq 5 \text{ GeV}$
$N_{\text{charged}}/\text{jet}$	≥ 2
ϑ_{jet}	$30^\circ - 150^\circ$

Table 2: Selection cuts applied to general events and to three-jet events.

($E_1 > E_2 > E_3$). These exact jet energies were calculated from the inter-jet angles assuming massless kinematics (see e.g. [12]). The quality of the selected two-jet events is guaranteed already by the event cuts.

Besides general three-jet topologies, mirror-symmetric three-jet topologies (defined by $\theta_3 - \theta_2 \leq 5^\circ$) are considered in later cross-checks. Symmetric three-jet topologies form a class of especially simple and clean three-jet topologies which we used extensively in previous studies [4,12,13]. Therefore, events with symmetric topologies are considered separately in order to compare the results obtained with this clean, but statistically limited class of events with the results obtained from events with more general topologies. Note, that the symmetric-event sample is almost completely included in the general sample. However, it allows the angular range to be extended to lower values of θ_1 .

Initially 3,150,000 events measured by DELPHI enter into the analysis. In total 1,797,429 Z events fulfill the above event cuts, of which 1,031,080 are accepted as two-jet events, 309,227 as general and 53,344 as symmetric three-jet events.

The charged-particle multiplicity in cones perpendicular to the event axis of a two-jet event or the event plane of a three-jet event has then been determined. Besides the cuts mentioned above it was required that the axis of the cones has a polar angle of at least 30° with respect to the beam in order to assure a sufficient acceptance for particle tracks.

The multiplicity has been corrected for the applied cuts and the limited detector acceptance and resolution by a multiplicative correction factor. Using simulated events this has been calculated as the ratio of the multiplicities of generated events to accepted events at the detector level. The events were generated with the JETSET 7.3 parton-shower model [14] as tuned to DELPHI data [15]. The influence of the magnetic field, detector material, signal generation and digitisation was simulated. The simulated data were then treated like the measured events.

It has already been shown [2,15], that the Monte Carlo model underestimates the production of particles at large angles with respect to the primary partons. Therefore, the hadron multiplicity in cones perpendicular to the two-jet event axis or the three-jet event plane has been reweighted with a small overall multiplicative correction. It was deduced from a comparison of data and simulation for two-jet events. After correction the model well describes the data and its dependences on the three-jet topology.

In particular, due to the 400 MeV momentum cut on the charged particles the correction factors obtained for the charged multiplicity in the cones are comparably big (~ 2), but vary only slightly with event topology. Moreover, in the important ratio of the mul-

tiplicity of three- and two-jet events the correction factors cancel to a large extent. The correction factor for the ratio N_3/N_2 is only ~ 0.9 . The stability of the acceptance correction has been tested by varying the selections imposed on charged-particle tracks shown in Table 1. In particular the lower momentum cut has been changed by ± 100 MeV. No significant change in the results was observed. Conservatively a 10% relative uncertainty of the respective acceptance correction is assumed to propagate to the quoted multiplicities or multiplicity ratios. As this uncertainty is expected to mainly change the normalisation of the multiplicities it is not included in the overall uncertainties shown in the figures. It is, however, considered in the results obtained from global fits of the data.

4 Results

Experimental results on the average charged-hadron multiplicities in cones are presented for cones perpendicular to the event axis in two-jet events and cones perpendicular to the event plane in three-jet events. Moreover the ratio of the cone multiplicities in three- and two-jet events is given as well as the momentum spectra in cones perpendicular to the plane of three-jet events.

The charged-hadron multiplicity in cones perpendicular to the event axis in two-jet events, N_2 , is given in Table 3 for three different cone opening angles and three different values of the jet-resolution parameter $y_{\text{cut}}^{\text{aoD}}$. The multiplicity shows the expected slight increase with y_{cut} and, due to the increase of phase-space, an approximately quadratic increase with cone opening angle.

The corresponding three-jet multiplicity, N_3 , is shown in Figure 1 as a function of the inter-jet angles θ_2 and θ_3 for general three-jet topologies and as a function of θ_3 for symmetric ones. The cone opening angle is $\vartheta_{\text{cone}} = 30^\circ$ and $y_{\text{cut}}^{\text{aoD}} = 0.015$. For the general three-jet events the bin width in θ_2 is: 2° for $98^\circ < \theta_2 < 108^\circ$, 3° for $108^\circ < \theta_2 < 111^\circ$, 4° for $111^\circ < \theta_2 < 123^\circ$ and 5° for $123^\circ < \theta_2 < 148^\circ$. The corresponding binning in θ_3 is: 10° for $120^\circ < \theta_3 < 140^\circ$ and 5° for $140^\circ < \theta_3 < 165^\circ$. For symmetric topologies the range in θ_1 is fixed by the highest accessible angle of 120° and the bin width of 5° imposed by the condition $\theta_3 - \theta_2 \leq 5^\circ$. The lower limit of $\theta_1 \sim 20^\circ$ depends on the applied value of y_{cut} . Numerical values of the results are given in [16]. The inner error bars represent the statistical error, the outer bars also include the systematic uncertainty relevant for the comparison to the theoretical expectation of Equation 1, added in quadrature. As only the ratio of multiplicities in three- and two-jet events enters in the comparison to the theoretical expectation (see Equation 1), the relative systematic uncertainty of the multiplicity has been taken to be identical to the relative error of the three- to two-jet

ϑ_{cone}	y_{cut}		
	0.01	0.015	0.02
20°	0.231 ± 0.001	0.245 ± 0.001	0.255 ± 0.001
30°	0.537 ± 0.001	0.570 ± 0.001	0.593 ± 0.001
40°	1.007 ± 0.002	1.067 ± 0.002	1.111 ± 0.002

Table 3: Charged-hadron multiplicity in cones perpendicular to the event axis in two-jet events, N_2 , as a function of the cone opening angle and the jet-resolution for the aoD algorithm. Errors are statistical.

multiplicity ratio. It has been determined as the r.m.s. of the results obtained when varying the cone size, jet-resolution and jet algorithm as described in Section 2.

The theoretical expectation, shown as a full line in Figure 1, describes the data well for all topologies except for large θ_3 for symmetric three-jet topologies. This region corresponds to small θ_1 , i.e. close-by low-energy jets. In this case the event plane is ill determined and data and theory cannot be compared reliably.

The prediction increases (by $\sim 7\%$, see dashed line in Figure 1) if the interference term of the theoretical prediction $\propto 1/N_c^2$ is omitted. In this case the prediction is significantly above the data.

In order to quantify this result the interference term in Equation 1 has been multiplied by an amplitude factor k and then fitted to the ratio N_3/N_2 of the multiplicities as given in Figure 1 and Table 3, respectively. The fit yields:

$$k = 1.37 \pm 0.05 \text{ (stat.)} \pm 0.33 \text{ (syst.)} \quad \chi^2/Ndf = 1.2$$

for general three-jet topologies and

$$k = 1.23 \pm 0.13 \text{ (stat.)} \pm 0.32 \text{ (syst.)} \quad \chi^2/Ndf = 2.1$$

for symmetric three-jet events with $\theta_1 > 48^\circ$. The systematic uncertainty of k was taken to be the r.m.s. of the results obtained when varying the cone size, jet-resolution and jet algorithm as described in Section 2. Moreover a 10% uncertainty on the acceptance correction applied for the multiplicity ratio has been assumed. The χ^2 has been calculated using statistical errors only. Therefore, a significant destructive interference term is observed in the data-to-theory comparison. The size of the term is consistent within error with expectation. Moreover it has been verified that the topology dependence of the $1/N_c^2$ term is consistent with that present in the data. This result represents the first direct verification of a colour suppressed negative antenna contribution not included in the usual probabilistic parton cascade calculation. Note, that it is based on the direct comparison of data to an absolute prediction. In particular no construction of an unphysical incoherent model is needed for the comparison.

Figure 2 a) shows the multiplicity ratio N_3/N_2 as function of r_t for different θ_3 . The data for different values of θ_3 agree well as is already expected from the good description of the data by the expectation, Equation 1, shown in Figure 1. The exclusive dependence on r_t as determined from the general-event sample is shown in Figure 2 b) compared to the expectation, i.e. to the homogeneous straight-line $N_3/N_2 = C_A/C_F \cdot r_t$ indicated dashed. The deviation of the points at low values of r_t is again due to events with close-by jets. A homogeneous straight line fit to the data for $r_t > 0.525$ yields for the slope:

$$2.211 \pm 0.014 \text{ (stat.)} \pm 0.053 \text{ (syst.)} \quad \chi^2/Ndf = 1.3$$

in astonishingly good agreement with the leading-order QCD expectation $C_A/C_F = 2.25$. The systematic uncertainty was again determined as for k in the interference term. The fit result is indicated by the full line in Figure 2 b). This result for the first time quantitatively verifies the colour-factor ratio C_A/C_F from hadronic multiplicities and a leading-order prediction. This simple prediction applies, because higher order contributions prove to be unimportant for soft particles emitted at large angles [7]. This is different from the more global case which depends on all the radiation inside jets. Moreover, these particles are least affected by energy-conservation and leading-particle effects.

For completeness it should be mentioned that the data do not allow the colour-factor ratio and the coherence term to be simultaneously verified due to the obvious high correlation of both terms. If such a fit is attempted the data can as well be described with

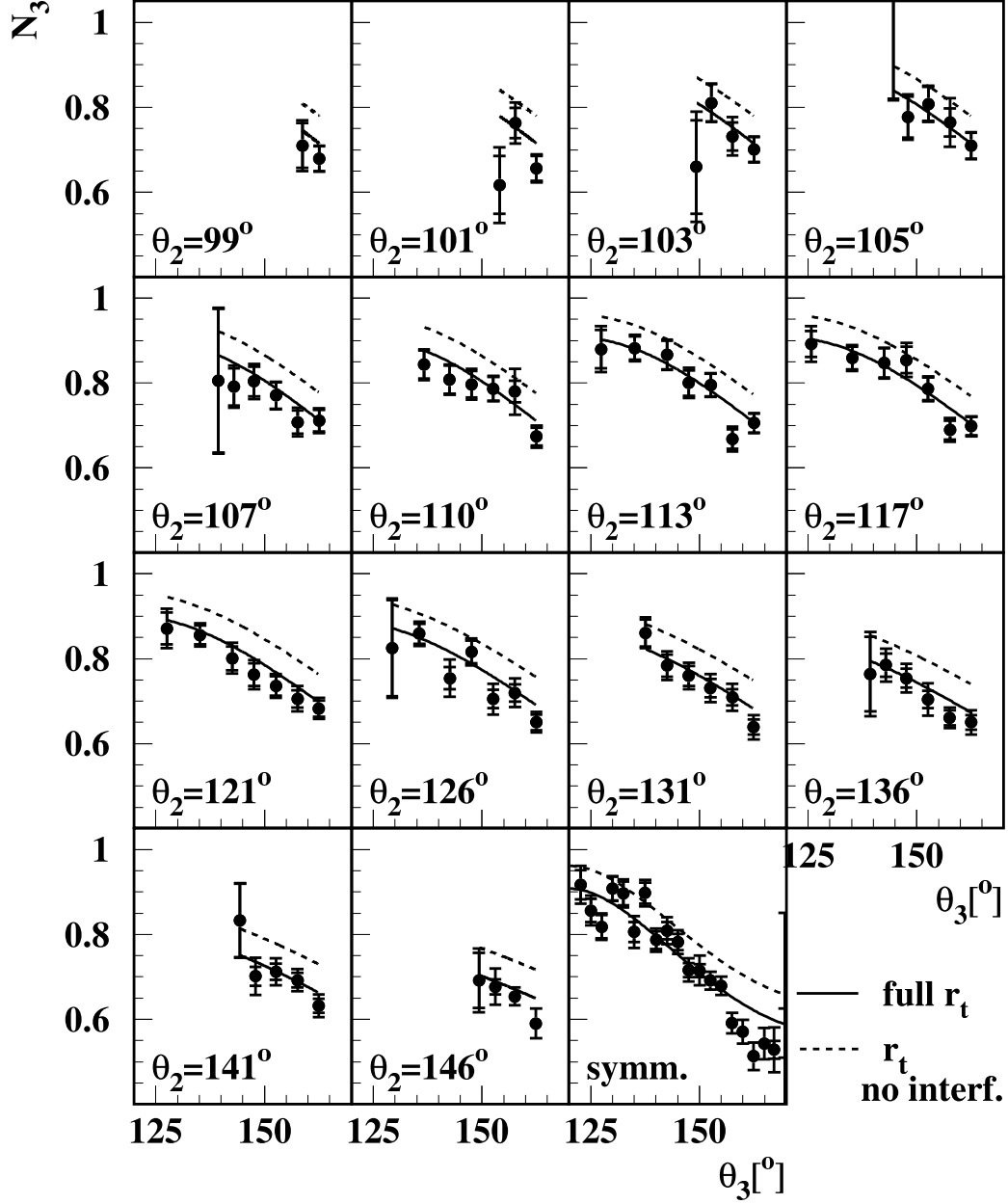


Figure 1: Multiplicity in cones of 30° opening angle perpendicular to the three-jet event plane, N_3 , as a function of the opening angles θ_2, θ_3 . The inner error bars are statistical, the outer also include systematic uncertainties (see text). The full line is the expectation deduced from Equation 1 using N_2 from Table 3. For the dashed line the interference term in Equation 1 ($\propto 1/N_c^2$) has been omitted.

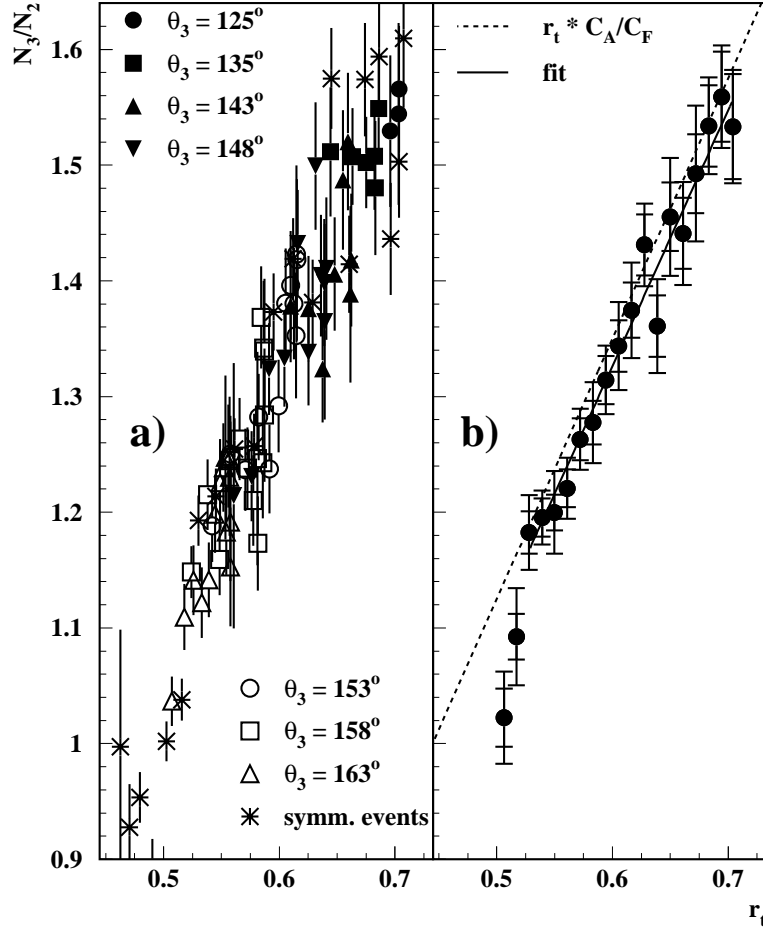


Figure 2: Multiplicity ratio N_3/N_2 in cones of 30° opening angle as function of r_t : a) for different angles θ_3 , errors are statistical; b) averaged over θ_3 , inner errors are statistical, outer errors include systematic uncertainties (see text). The dashed line is the expectation Equation 1, the full line is a fit to the data in the indicated r_t -interval.

$C_A/C_F \sim 2$ and $N_C \rightarrow \infty$. This result is also expected from gauge theories with a large number of colours. It is clear, however, that this solution does not apply as $N_C = 3$ is well known experimentally, e.g. from the ratio, R , of the hadronic to the leptonic cross-section at the Z pole.

The dependence of the multiplicity on the scale r_t only allows inclusive distributions of the produced hadrons to be studied. In Figure 3 a) the differential momentum distribution is shown for different values of r_t . The momentum distributions are observed to scale approximately with r_t . This is most clearly seen in Figure 3 b) where the ratio of the momentum spectra to the average spectrum is shown. Moreover, these ratios have been scaled by $\langle r_t \rangle / r_t$ such that a unit value for the overall multiplicity ratio is expected. For small momenta ($p < 1$ GeV) the data are consistent with unity, for higher momenta less (more) particles are produced for small (high) scales r_t , respectively. The constancy of the ratio is expected if the production of hadrons is directly proportional to gluon radiation, thus the observed result strongly supports the conjecture of local parton-hadron duality, LPHD [17], for low-energy hadrons. The deviation from unity for higher momenta may be understood as being due to the increase of the hadronic phase-space for high r_t .

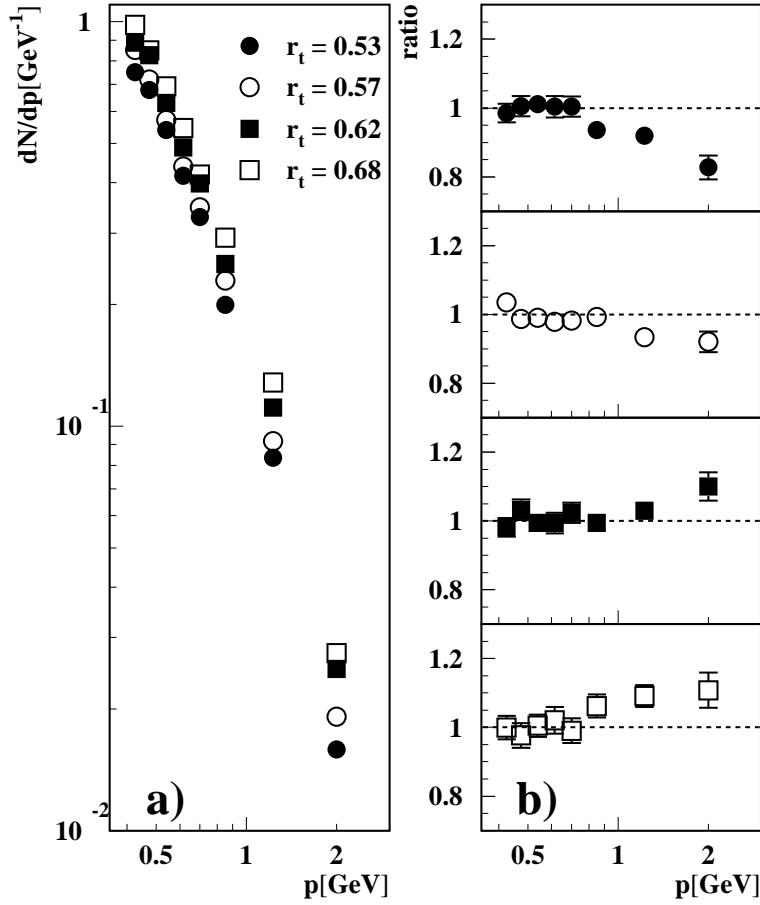


Figure 3: a) Differential momentum distribution of hadrons in cones of 30° opening angle perpendicular to the three-jet event plane for different values of r_t (aoD algorithm, $y_{cut} = 0.015$). b) Ratio of the momentum distributions to their average reweighted using Equation 1 and the individual r_t values.

In summary the multiplicity in cones perpendicular to the event plane of three-jet events produced in e^+e^- annihilation has been measured for the first time and compared to the corresponding multiplicity in two-jet events. The multiplicity ratio is well described by a leading-order QCD prediction also including a destructive interference term. The presence of destructive interference and thereby of the coherent nature of soft hadron production was verified from the comparison of the data to the absolute QCD prediction. The slope of the hadron multiplicity with the topological variable r_t directly represents the colour-factor ratio C_A/C_F . This measurement for the first time is able to verify the colour-factor ratio using a hadron multiplicity measurement and a leading-order QCD prediction. This possibility is a consequence of the favorable perturbative situation studied and the focus on low-energy large-angle particles. A simultaneous study of the momentum and topology dependence of the hadron multiplicity provides evidence for the LPHD conjecture.

Acknowledgements

We are greatly indebted to our technical collaborators, to the members of the CERN-SL Division for the excellent performance of the LEP collider, and to the funding agencies for their support in building and operating the DELPHI detector.

We acknowledge in particular the support of

Austrian Federal Ministry of Education, Science and Culture, GZ 616.364/2-III/2a/98, FNRS-FWO, Flanders Institute to encourage scientific and technological research in the industry (IWT), Belgium,

FINEP, CNPq, CAPES, FUJB and FAPERJ, Brazil,

Czech Ministry of Industry and Trade, GA CR 202/99/1362,

Commission of the European Communities (DG XII),

Direction des Sciences de la Matière, CEA, France,

Bundesministerium für Bildung, Wissenschaft, Forschung und Technologie, Germany,

General Secretariat for Research and Technology, Greece,

National Science Foundation (NSF) and Foundation for Research on Matter (FOM),

The Netherlands,

Norwegian Research Council,

State Committee for Scientific Research, Poland, SPUB-M/CERN/PO3/DZ296/2000,

SPUB-M/CERN/PO3/DZ297/2000, 2P03B 104 19 and 2P03B 69 23(2002-2004)

FCT - Fundação para a Ciência e Tecnologia, Portugal,

Vedecká grantová agentúra MS SR, Slovakia, Nr. 95/5195/134,

Ministry of Science and Technology of the Republic of Slovenia,

CICYT, Spain, AEN99-0950 and AEN99-0761,

The Swedish Natural Science Research Council,

Particle Physics and Astronomy Research Council, UK,

Department of Energy, USA, DE-FG02-01ER41155.

EEC RTN contract HPRN-CT-00292-2002.

We thank V. Khoze and W. Ochs for numerous enlightening discussions and helpful explanations and comments.

References

- [1] V. A. Khoze and W. Ochs, Int. J. Mod. Phys. **A 12** (1997) 2949 [arXiv:hep-ph/9701421].
- [2] I. G. Knowles *et al.*, “QCD Event Generators”, in “Physics at LEP II”, CERN 96-01, Vol. 2, p. 103 [arXiv:hep-ph/9601212].
- [3] E. R. Boudinov, P. V. Chliapnikov and V. A. Uvarov, Phys. Lett. **B 309** (1993) 210.
- [4] DELPHI Collab. P. Abreu *et al.*, Z. Phys. **C 70** (1996) 179.
- [5] Y. L. Dokshitzer *et al.*, “Basics Of Perturbative QCD”, Edition Frontières, Gif sur Yvette, 1991.
- [6] Y. I. Azimov *et al.*, Phys. Lett. **B 165** (1985) 147.
- [7] V. A. Khoze, S. Lupia and W. Ochs, Phys. Lett. **B 394** (1997) 179 [arXiv:hep-ph/9610204], Eur. Phys. J. **C 5** (1998) 77 [arXiv:hep-ph/9711392].
- [8] Y. L. Dokshitzer *et al.*, JHEP **9708** (1997) 001 [arXiv:hep-ph/9707323].
- [9] S. Catani *et al.*, Phys. Lett. **B 269** (1991) 432.
- [10] DELPHI Collab. P. A. Aarnio *et al.*, Nucl. Instrum. Meth. **A 303** (1991) 233.
- [11] DELPHI Collab. P. Abreu *et al.*, Nucl. Instrum. Meth. **A 378** (1996) 57.
- [12] DELPHI Collab. P. Abreu *et al.*, Eur. Phys. J. **C 13** (2000) 573.

- [13] DELPHI Collab. P. Abreu *et al.*, Phys. Lett. **B 449** (1999) 383 [arXiv:hep-ex/9903073].
- [14] T. Sjöstrand, CERN-TH.7112-93 (rev.) [arXiv:hep-ph/9508391].
- [15] DELPHI Collab. P. Abreu *et al.*, Z. Phys. **C 73** (1996) 11.
- [16] M. Siebel, Dissertation, Bergische Univ. Wuppertal, WUB-DIS 2003-11,
<http://elpub.bib.uni-wuppertal.de/edocs/dokumente/fbc/physik/diss2003/siebel/>.
- [17] Y. I. Azimov *et al.*, Z. Phys. **C 27** (1985) 65, Z. Phys. **C 31** (1986) 213.